

Development of ASURA I: Harvestman-like Hexapod Walking Robot -Approach for Long-legged Robot and Leg Mechanism Design-

Ryuichi Hodoshima¹, Soichiro Watanabe¹, Yuki Nishiyama¹,
Akihiro Sakaki¹, Yoshikazu Ohura¹ and Shinya Kotosaka¹

Abstract—In this paper, a harvestman-like hexapod walking robot named ASURA I is proposed and its leg mechanism design is discussed. Modeled on a harvestman in nature, the authors have introduced the concept of mobile form that has long legs and small body to ASURA I to enhance mobile performance on rough terrain. To develop long legs relative to body, special parallel link mechanism to drive leg joints powerfully and effectively is introduced to leg mechanism of ASURA I. First, we discuss design problems of leg mechanism in detail: leg length, DOF configuration, actuator selection and leg driving system. Then, analysis of kinematics, singularity and static characteristic of leg mechanism are reported. Finally, the prototype leg, which is 1.3 m in length and 3.2 kg in weight, has been developed and tested on some basic performance. The prototype successfully have demonstrated very basic motion.

I. INTRODUCTION

Five major characteristics of legged-robots are the following:

- 1) Free selection of supporting points on ground surface
- 2) Function of forming discrete support points
- 3) Function of reducing pressure on ground contact surfaces
- 4) Non-slip turnabout function
- 5) Functions of building secure and active scaffolds

For these widespread strong points, a lot of studies on walking robots have been reported for many decades [1]–[4]. It is pointed out that the insect type leg is suitable for walking on rough terrain [5], [6]. In the insect type leg, its knee joint is located laterally or higher than its hip and the configuration is sprawling wide-track. Long legs are applicable to the insect type configuration by keeping the body's center of gravity lower and in maintaining high stability. The introduction of long legs enables walking robots to walk faster and is adaptive to comparatively large unevenness of the ground.

However, leg mechanisms of conventional walking robots are not long as compared to its body length with no relation to the robot size, because of poor performance of actuator and low stiffness of leg structure. In addition, walking robots equipped with long legs has big or long trunk when compared with their legs, and big or long trunk hampers their walking motion. So it can be concluded that walking robots should have small body and long legs to enhance mobile performance on rough terrain. In other words, walking robot with long legs relative to robot body size has great potential in traversing irregular terrains.

*This work was supported by SUZUKI Foundation and Okumura Corporation.

¹R. Hodoshima, S. Watanabe, Y. Nishiyama, A. Sakaki, Y. Ohura and S. Kotosaka are with Department of Mechanical Engineering, Saitama University, 255 Shimo-Ohkubo, Sakura-ku, Saitama-shi, Saitama, 338-8570, Japan hodoshima at mech.saitama-u.ac.jp



Fig. 1. Real harvestman

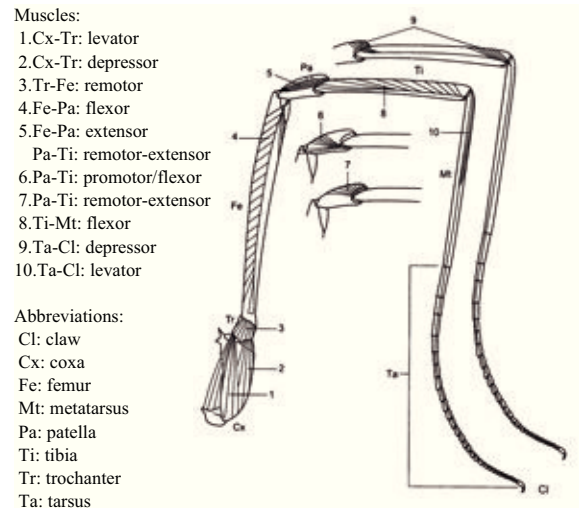


Fig. 2. Detail of real harvestman leg [7]

In the present study, we aim to develop a walking robot equipped with long legs relative to body for realization of high-performance mobility on rough terrain. For the realization of the robot, we model a harvestman in nature that walks on a rocky area, tree, sandy soil, and so on actively to construct a hexapod walking robot by developing long legs and a small body. In this paper, we report the following items: concept of the robot; leg mechanism design; analyses of kinematics; singularity and static characteristic; basic experiments.

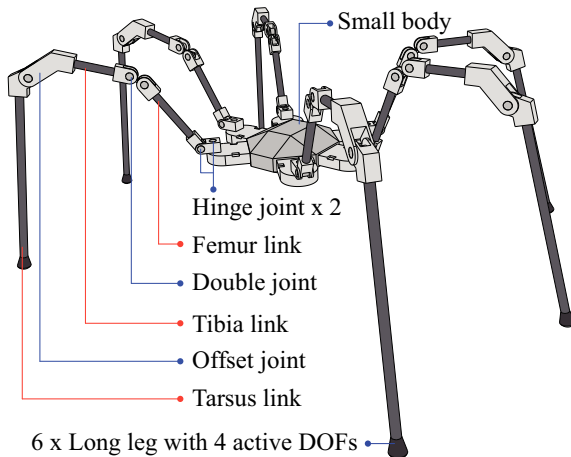


Fig. 3. Concept of ASURA I

II. ASURA I: HARVESTMAN-LIKE HEXAPOD WALKING ROBOT

A. Characteristic of Harvestman

As shown in Fig.1, a real harvestman has long legs relative to its body. The following items can be listed as external characteristic of a harvestman [7]:

- 1) Body is composed of the cephalothorax and abdomen and appears to be a single oval structure.
- 2) Harvestman has six pairs of appendages, a pair of chelicerae, a pair of pedipalps, four pairs of legs. The second pair of legs are longer than the others and not used for walking; they function as antennae or feelers.
- 3) Harvestman usually walks in tripod gait or wave gait.

The leg configuration of harvestman is shown in Fig.2. Even though there is a certain amount of differences in leg configuration according to the types of harvestman, a common characteristic of harvestman's leg is as follows:

- 1) Leg consists of seven segments: coxa, trochanter, femur, patella, tibia, metatarsus and tarsus.
- 2) Joints located near the body appears to be ball-joint or universal-joint and joints far from knee joint appears to be hinge joint.
- 3) Tarsus is composed of multi segments and flexible structure.

B. Harvestman-like hexapod walking robot: ASURA I

From an above-mentioned characteristic of harvestman and the reports [8], [9], we propose a harvestman-like hexapod walking robot "ASURA I" as shown in Fig.3 and the robot characteristic is as follows:

- 1) By reducing a number of DOFs of leg mechanism than that of a real harvestman, the number is four. All joints are revolute.
- 2) Pseudo double joint is introduced to the knee joint to make the motion range larger.
- 3) Offset joint is applied to the tibia joint to extend the horizontal motion range of toe tip for walking.
- 4) All legs are positioned radially around the body for omni-directional motion.

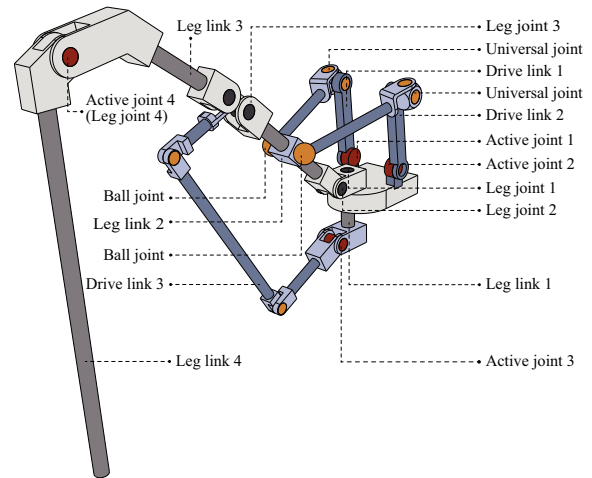


Fig. 4. Concept of leg mechanism and DOF configuration

- 5) The ratio of the length of leg to that of body is four to one, after taking into account the physical characteristics of both real harvestman and conventional legged robots.
- 6) Toe mechanism would be introduced, which consists of multi linkage to improve terrain-adaptability.

III. LEG MECHANISM DESIGN

A. Concept of leg mechanism

To construct a legged robot that has long legs relative to its body, leg mechanism is requested: to support its own weight at the point far from body; to have the large workspace of the leg tip; to be highly rigid structure. To negotiate these problems, "coupled drive [10], [11]" is introduced, which couples the multiple actuators of the robot system as much as possible in the normal driving mode and let them produces the power cooperatively.

The leg mechanism is designed by introducing the coupled drive and parallel link mechanism. The concept is shown in Fig.4. The leg mechanism is composed of two type links, one is the leg link as a leg born to support the robot's own weight and another is a drive link as a leg muscle to drive leg joints. The leg joint 1 and 2 are driven by the drive link 1 and 2, the leg joint 3 is driven by the drive link 3, respectively. Only the leg joint 4 is driven directly by the actuator 4.

Taking account of size and weight of actuators, batteries and robot body, specification of leg mechanism was determined as follows:

- 1) The target weight and length are 3.0 kg and 1.3 m.
- 2) The motion range of each joint is maximized as much as possible.
- 3) Each leg mechanism is modularized.
- 4) Actuators for all joints are DC servo motor.
- 5) CFRP pipes are used as the leg links for weight saving and rigidity.

B. Leg joint 1 and 2

The leg joint 1 and 2 are composed of two passive joints: yaw axis and pitch axis, respectively. As already described, the leg joint 1 and 2 are driven by the drive link 1 and 2.

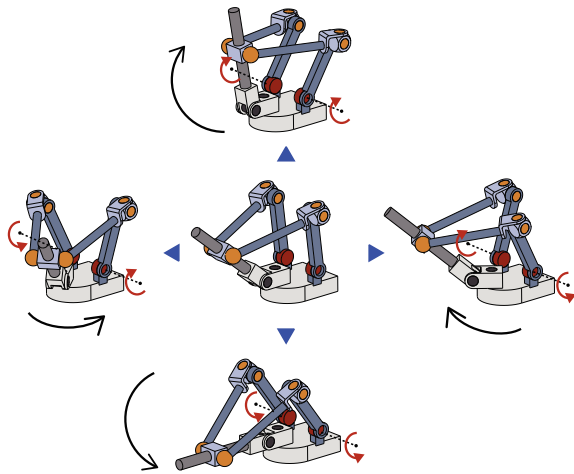


Fig. 5. Drive concept of leg joint 1 and 2

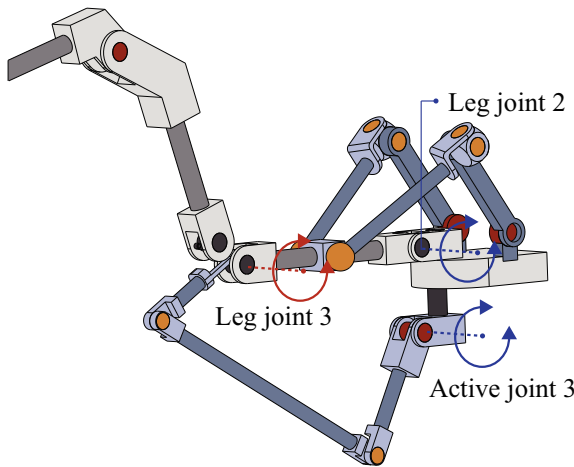


Fig. 6. Drive concept of leg joint 3

Driving these left and right links can constitute coupled drive to create 2-DOF-motions (Fig.5). Each drive link is composed of a driven arm and a driving arm equipped with active rotational joint. The driven arm is connected to the driving arm and the leg link 2 via universal joint and ball joint, respectively. The universal joint and ball joint are designed by combining two or three passive rotational joints and these joints have wider motion range than commercially available joints. The drive link system has six DOFs and bending moments acting on passive joints are zero. Therefore, only forces of compression and tension are applied to the driven arm and structural parts could be down-sized. Besides, the introduction of linkage mechanism could reduce the moment of inertia around the leg joint 1 because heavy actuators are placed near the body.

C. Leg joint 3

As shown in Fig.4 and Fig.6, the angle of leg joint 3 is determined by the drive link 3 and the leg link 2. This means the leg joint 3 is driven by the actuator 1, 2 and 3. As well as the leg joint 1 and 2, an actuator for the drive link 3 is placed near the body and this reduces the moment of inertia around the leg joint 1. Pseudo double joint is introduced to

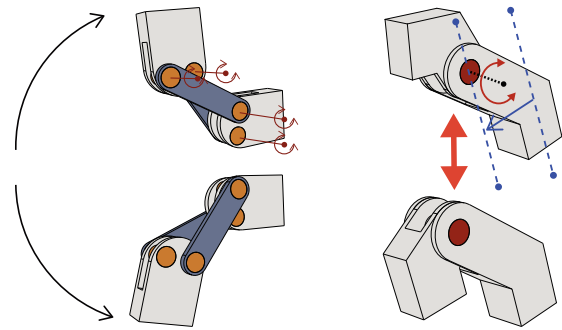


Fig. 7. Double joint

Fig. 8. Offset joint

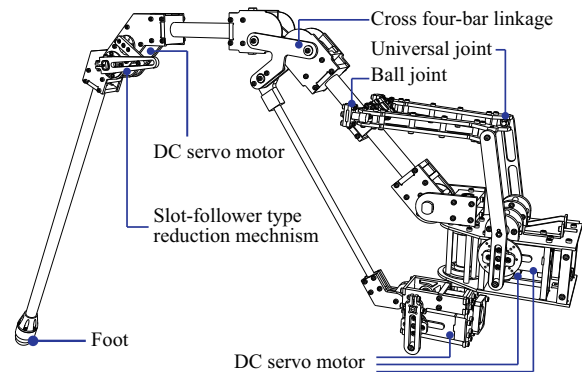


Fig. 9. Drawing of leg mechanism by 3D CAD

the leg joint 3 (the knee joint) by emulating the structure of a real harvestman's leg for the purpose of extending the motion range. The pseudo double joint is composed of cross four-bar linkage mechanism as shown in Fig.7. Actually, the pseudo double joint is driven by the drive link 3.

D. Leg joint 4

The leg joint 4 is not required to generate large torque as the other joints do, but need to have wide motion range for swing leg motion. Therefore, we make the leg joint 4 driven directly by the actuator 4. As shown in Fig.8, the offset joint is applied to the leg joint 4 for the leg mechanism to have wide workspace in the direction of the body side.

E. Actual design

From the above discussions, actual mechanism of the leg mechanism was designed using 3D-CAD Pro/ENGINEER Wildfire 5.0. the prototype leg 3.2 kg in weight and 1.3 m in length as shown in Fig.15. The joints are mainly made of aluminium alloys (A5052) and CFRP pipes are used as the leg links. All actuators are DC servo motors (VS-SV1150; Vstone Co. Ltd.). The driving arms are driven by the motors via reduction mechanism that is composed of slot and follower. The shape of the leg tip is dome, which is made of urethane.

IV. LEG MECHANISM ANALYSIS

A. Kinematics

The kinematics related to only leg links and leg joint is similar to that of the conventional serial link manipulator. Thus, the kinematics of the leg joints and the actuators is discussed in this section.

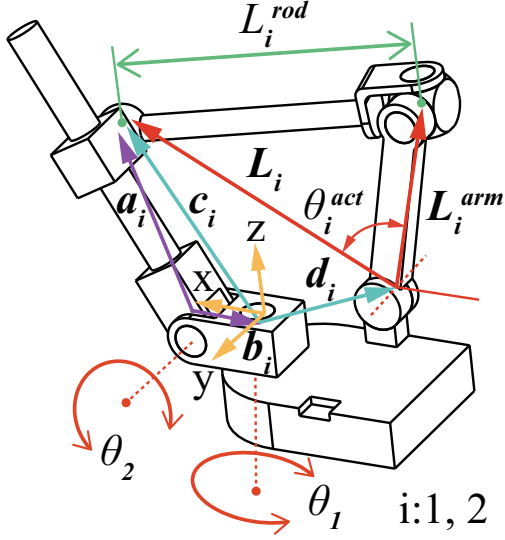


Fig. 10. Kinematics model of leg joint 1 and 2

1) *Leg joint 1 and 2*: Fig.10 shows the kinematics model of the leg joint 1 and 2. This parallel link mechanism constitutes the closed loop system and is subject to geometric constraint. Therefore, we develop the conditional expression for the closed loop system. First, we focus on the closed loop system on one side. Notations, depicted in Fig.10, are listed as follows:

- \mathbf{a}_i is the position vector from the leg joint 2 to the ball joint
- \mathbf{b}_i is the position vector from the leg joint 2 to the leg joint 1
- \mathbf{c}_i is the position vector from the leg joint 1 to the ball joint
- \mathbf{d}_i is the position vector from the leg joint 1 to the actuator
- \mathbf{L}_i is the position vector from the actuator to the ball joint
- \mathbf{L}_i^{arm} is the position vector from the actuator to the universal joint
- L_i^{rod} is the length between the ball joint and the universal joint

The component of a vector is described using index notation such as $\mathbf{L}_i = (L_{ix}, L_{iy}, L_{iz})$. Using these parameters, the position vector \mathbf{c}_i and \mathbf{L}_i are given by

$$\mathbf{c}_i = \mathbf{E}^{j\theta_2} \mathbf{a}_i - \mathbf{b}_i \quad (1)$$

$$\mathbf{L}_i = \mathbf{E}^{k\theta_1} \mathbf{c}_i - \mathbf{d}_i \quad (2)$$

where $\mathbf{E}^{n\theta}$ ($n = i, j, k$) is a rotation matrix around the n axis. The conditional expression for the closed loop system can be expressed using following formula.

$$f_i = (\mathbf{L}_i - \mathbf{L}_i^{arm})^2 - (L_i^{rod})^2 = 0 \quad (3)$$

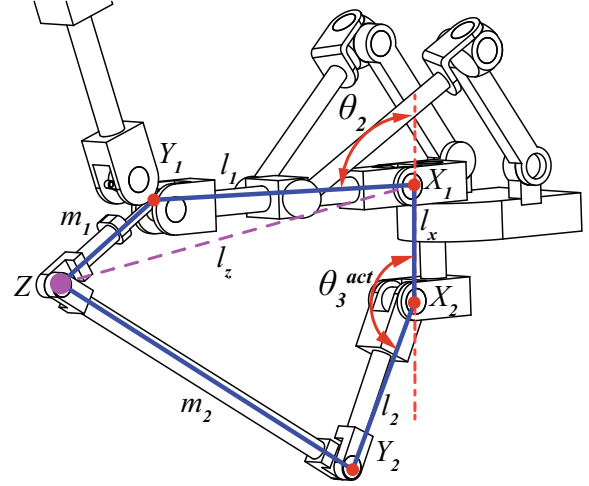


Fig. 11. Kinematics model of leg joint 3

By solving Eq.3 for actuator angle, θ_i^{act} is obtained by

$$\theta_i^{act} = \sin^{-1} \frac{X^2 + Y^2 + Z^2 - (L_i^{rod})^2}{2XY} - \phi \quad (4)$$

$$X = \sqrt{(L_{ix})^2 + (L_{iz})^2}$$

$$Y = \sqrt{(L_{ix}^{arm})^2 + (L_{iz}^{arm})^2}$$

$$Z = (L_{iy} - L_{iy}^{arm})^2, \phi = \cos^{-1} \frac{L_{iz}}{X}$$

2) *Leg joint 3*: Fig.11 shows the kinematics model of the leg joint 3. Angle of the leg joint 3 is determined by the leg link 2 and the drive link 3; the leg link 2 is driven by the actuator 1 and 2, and the drive link 3 is driven by the actuator 3. If angle of the leg joint 3 is given, we can get the position of \mathbf{Z} depicted in Fig.11. Thus, the conditional expression for this closed loop system can be expressed using following formula as well as the leg joint 1 and 2.

$$(\mathbf{Z} - \mathbf{Y}_i)^2 - m_i^2 = 0 (i = 1, 2) \quad (5)$$

By solving Eq.5 for the actuator angle, θ_3^{act} is given by

$$\theta_3^{act} = \sin^{-1} \frac{l_2^2 + Z_x^2 + Z_y^2 + n^2 - m_2^2}{|\mathbf{Z}|} - \psi \quad (6)$$

$$n = Z_z + l_z, \psi = \sin^{-1} \frac{n}{|\mathbf{Z}|}$$

B. Singularity

1) *Leg joint 1 and 2*: Here, let $\boldsymbol{\theta}_S = (\theta_1, \theta_2)^T$, $\boldsymbol{\theta}_A = (\theta_1^{act}, \theta_2^{act})^T$ and differentiating Eq.3 with respect to time gives the following expression.

$$\mathbf{J}_A \dot{\boldsymbol{\theta}}_A + \mathbf{J}_S \dot{\boldsymbol{\theta}}_S = 0 \quad (7)$$

From Eq.7, the following two kinds of Jacobian matrices are obtained:

$$\mathbf{J}_A = \begin{pmatrix} 2(\mathbf{L}_1 - \mathbf{L}_1^{arm}) \frac{\partial \mathbf{L}_1}{\partial \theta_1^{act}} & 0 \\ 0 & 2(\mathbf{L}_2 - \mathbf{L}_2^{arm}) \frac{\partial \mathbf{L}_2}{\partial \theta_2^{act}} \end{pmatrix} \quad (8)$$

$$\mathbf{J}_S = \begin{pmatrix} 2(\mathbf{L}_1 - \mathbf{L}_1^{arm}) \frac{\partial \mathbf{L}_1}{\partial \theta_1} & 2(\mathbf{L}_1 - \mathbf{L}_1^{arm}) \frac{\partial \mathbf{L}_1}{\partial \theta_2} \\ 2(\mathbf{L}_2 - \mathbf{L}_2^{arm}) \frac{\partial \mathbf{L}_2}{\partial \theta_1} & 2(\mathbf{L}_2 - \mathbf{L}_2^{arm}) \frac{\partial \mathbf{L}_2}{\partial \theta_2} \end{pmatrix} \quad (9)$$

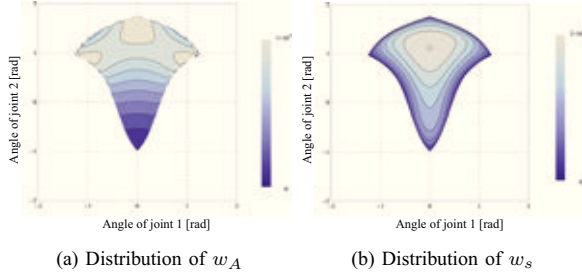


Fig. 12. Relationship between Euclidean norm of Jacobian matrix, leg joint 1 and 2

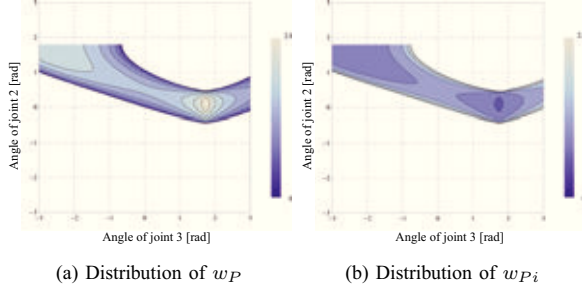


Fig. 13. Relationship between Euclidean norm of Jacobian matrix, leg joint 2 and 3

Here, it is reported in ref. [12], [13] that: the first type of singularity occurs when $rank \mathbf{J}_A < dim \theta_S$; the second type of singularity occurs when $rank \mathbf{J}_S < dim \theta_S$; the third type of singularity occurs when both the first and second type of singularities is involved. Let us compute Euclidean norm of Eq.8 and 9 to investigate the singularity. Euclidean norms of \mathbf{J}_A and \mathbf{J}_S are given by

$$w_A = \sqrt{\det|\mathbf{J}_A^T \mathbf{J}_A|}, w_S = \sqrt{\det|\mathbf{J}_S^T \mathbf{J}_S|} \quad (10)$$

w_A and w_S approach zero when being near singularity. Thus, we computed w_A and w_S within whole motion range of the leg mechanism. The results of computing w_A and w_S are shown in Fig.12. In the figures, dark-colored points are close to singularity. w_A and w_S approach zero in the boundary of the motion range of θ_1 and θ_2 . So it has been confirmed that singularity dose not exist in the movable range and have little influence on leg motion.

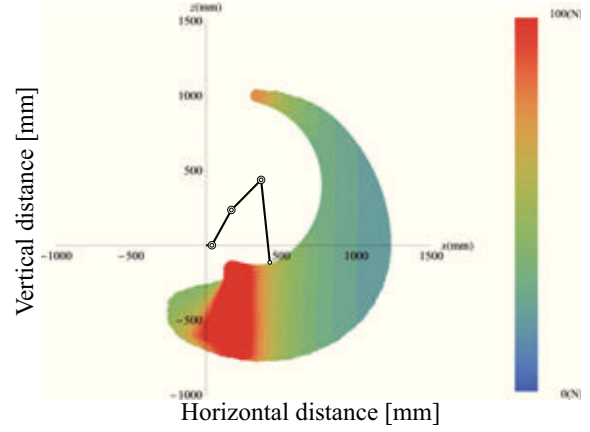
2) *Leg joint 3*: Driving mechanism for the leg joint 3 is essentially similar to five-bar linkage mechanism driven by the leg joint 2 and the actuator 3. Therefore, a relation between the angular velocity of the leg joint 3, that of the leg joint 2 and that of the actuator 3 can be expressed using following formula.

$$\dot{\theta}_3 = \mathbf{J}_P(\dot{\theta}_2, \dot{\theta}_3^{act})^T \quad (11)$$

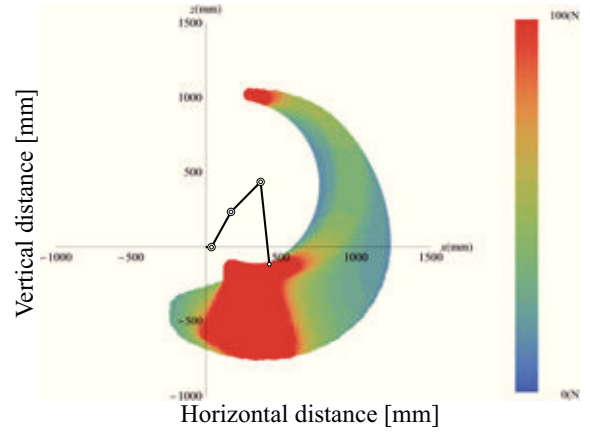
The following Euclidean norm w_P and w_{P_i} approach zero when being near singularity as well as the joint 1 and 2. w_P and w_{P_i} can be expressed as

$$w_P = \sqrt{\det|\mathbf{J}_P^T \mathbf{J}_P|}, w_{P_i} = \sqrt{\det|(\mathbf{J}_P^{-1})^T \mathbf{J}_P^{-1}|} \quad (12)$$

we calculated w_P and w_{P_i} within whole motion range of the leg mechanism, and the results are plotted in Fig.13. In the figures, dark-colored points are close to singularity, too.



(a) Conventional mechanism that each actuator is mounted to each joint and drives the joint directly



(b) Coupled drive mechanism that actuators produce the power cooperatively

Fig. 14. Output force distribution to the downward at the tip of the leg mechanism

w_P approaches zero in the boundary of the motion range of θ_2 and θ_3 . There are the points that w_{P_i} approaches zero in the movable range. However, it has been confirmed that self-collision of the leg structure would occur at such points and the singularity had no influence on the leg motion.

C. Static characteristic

The relationship between the position of the leg tip and angles of the actuators is expressed as

$$\dot{\mathbf{P}} = \mathbf{J} \dot{\theta}_{act} \quad (13)$$

$$\mathbf{J} = \begin{pmatrix} \frac{\partial x}{\partial \theta_1} & \frac{\partial x}{\partial \theta_2} & \frac{\partial x}{\partial \theta_3} & \frac{\partial x}{\partial \theta_4} \\ \frac{\partial y}{\partial \theta_1} & \frac{\partial y}{\partial \theta_2} & \frac{\partial y}{\partial \theta_3} & \frac{\partial y}{\partial \theta_4} \\ \frac{\partial z}{\partial \theta_1} & \frac{\partial z}{\partial \theta_2} & \frac{\partial z}{\partial \theta_3} & \frac{\partial z}{\partial \theta_4} \end{pmatrix} \begin{pmatrix} \frac{\partial \theta_1}{\partial \phi_1} & \frac{\partial \theta_1}{\partial \phi_2} & 0 & 0 \\ \frac{\partial \theta_2}{\partial \phi_1} & \frac{\partial \theta_2}{\partial \phi_2} & 0 & 0 \\ \frac{\partial \theta_3}{\partial \phi_1} & \frac{\partial \theta_3}{\partial \phi_2} & \frac{\partial \theta_3}{\partial \phi_3} & 0 \\ 0 & 0 & 0 & \frac{\partial \theta_4}{\partial \phi_4} \end{pmatrix} \quad (14)$$

where $\mathbf{P} = (x, y, z)$ is the position vector of the leg tip, $\phi_i = \theta_i^{act}$ is the angle of i -th actuator. The relation between torque of the actuators and force of the leg mechanism is obtained from the principle of virtual work, $\boldsymbol{\tau} = \mathbf{J}^T \mathbf{F}$, where $\boldsymbol{\tau}$ denotes torque of the actuator and \mathbf{F} does the force of the leg mechanism.

The computing results are shown in Fig.14. In this case, the angle of the leg joint 1 is zero rad in Fig.14(b). For

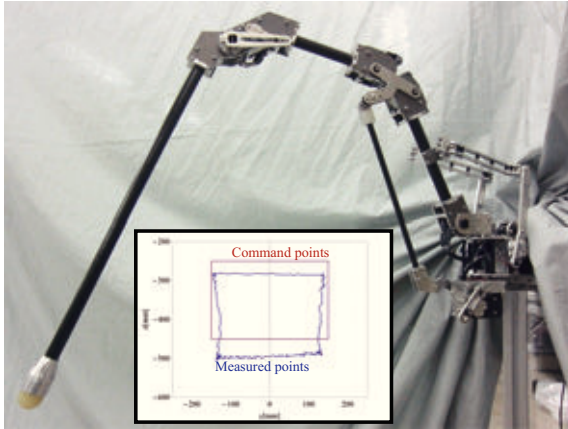


Fig. 15. Leg prototype and result of continuous path experiment

ease in comparison, we make the movable range of joints in Fig.14(a) equal to that of joints in Fig.14(b). From Fig.14, the effect of coupled drive makes the output force of the leg more powerful than that of the conventional leg mechanism in which the leg joints are driven individually.

V. EXPERIMENT

We conducted the continuous path experiment with this prototype. The motion trajectory was the rectangle 0.4 m in width and 0.2 m in height, which is the planned trajectory for swing leg when the robot walks. The position command was sent to all motors from PC (OS: Windows7 Professional 64bit) during the experiment.

Experiment result are shown in the bottom figure of Fig.15. From this experiment result, it can be confirmed that there was the position error between the target and the measured trajectory. The error was about 40 mm, which is about 3 percent of leg length. We expected to have failed to conduct sufficient parameter tuning of self-weight compensation and PID controller for DC servo motors.

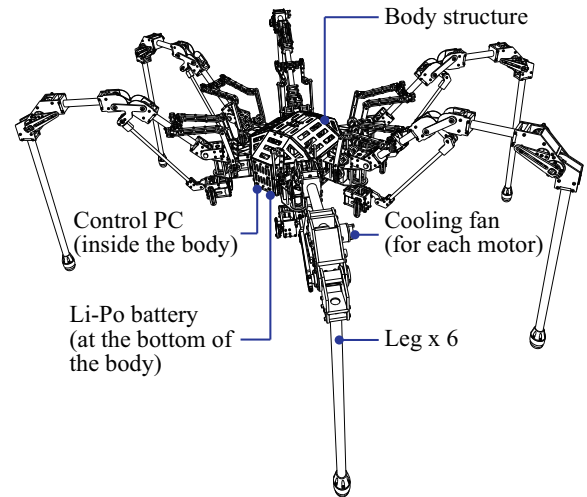
VI. CONCLUSIONS

In this paper, we proposed a novel hexapod walking robot for improving the mobility on the rough terrain inspired by a harvestman in nature. Leg mechanism was also proposed using coupled drive and parallel link mechanism and expected to have powerful output and wide motion range. Then, kinematics, singularity and static characteristic were investigated. Moreover, the prototype leg was developed and verified through the continuous path experiment.

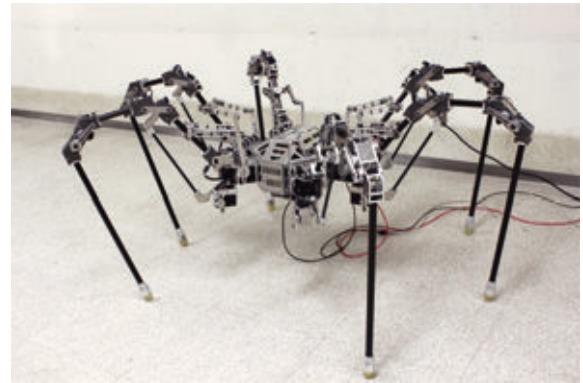
In addition, we have designed the body and system architecture of ASURA I as shown in Fig.16(a). We have been developing the prototype of ASURA I (Fig.16(b)). We are planning to conduct the walking experiment on level terrain using the prototype of ASURA I. After that, walking experiments will be carried out on highly rough terrain.

REFERENCES

- [1] Waldron, K.J. and McGhee, R.B., "The Adaptive Suspension Vehicle," IEEE Control Systems Magazine, Vol.6, No.6, pp.7-12, 1986.
- [2] B. Gassmann, K. U. Scholl, K. Berns, "Behaviour control of Lauron III for walking in unstructured terrain," Proc. of Climbing and Walking Robots, pp.651-658, 2001.



(a) 3D mockup of ASURA I



(b) Constructed prototype of ASURA I

Fig. 16. ASURA I

- [3] T. Takubo, T. Arai, K. Inoue, H. Ochi, T. Konishi, T. Tsurutani, Y. Hayashibara, E. Koyanagi, "Integrated Limb Mechanism Robot ASTERISK," J. of Robotics and Mechatronics, Vol.18, No.2, pp.203-214, 2006.
- [4] P. Gonzalez de Santos, J. A. Cobano, E. Garcia, J. Estremera, M.A. Armada, "A six-legged robot-based system for humanitarian demining missions," Mechatronics, Vol. 17, pp. 417-430, 2007.
- [5] S. Hirose, Y. Umetani, "The basic motion regulation system for a quadruped walking vehicle," ASME 80-DET-34, 1980.
- [6] D. C. Kar, "Design of Statically Stable Walking Robot; A Review," J. of Robotic Systems, Vol. 20, No.11, pp.671-686, 2003.
- [7] R. Pinto-da-Rocha, G. Machado, G. Giribet, "HARVESTMAN: The Biology of Opiliones," Harvard University Press, 2007.
- [8] E. F. Fichter, B.L. Fichter, "A Survey of Legs of Insects and Spiders From a Kinematics Perspective," Proc. of IEEE Int. Conf. on Robotics and Automation, pp.984 -986, 1988.
- [9] A. Gasparetto, R. Vidoni, T. Seidl, "Kinematic study of the spider system in a biomimetic perspective," Proc. of IEEE/RSJ Int. Conf. on Intelligent Robots and Systems, pp.3077-3082, 2008.
- [10] S. Hirose, M. Sato, "Coupled drive of the multi-DOF robot," Proc. of IEEE Int. Conf. on Robotics and Automation, pp.1610-1616, 1989.
- [11] Y. Sugahara, N. Yonezawa, K. Kosuge, "A Novel Stair-Climbing Wheelchair with Transformable Wheeled Four-Bar Linkages," Proc. of IEEE/RSJ Int. Conf. on Intelligent Robots and Systems, pp.3333-3339, 2010.
- [12] C. Gosselin and J. Angeles, "Singularity Analysis of Closed-Loop Kinematic Chains," IEEE Trans. on Robotics and Automation, Vol.6, No.3, pp.281-290, 1990.
- [13] B. M. St-ongue, C. Gosselin, "Singularity Analysis and Representation of Spatial Six-dof Parallel Manipulators," Recent Advances in Robot Kinematics, pp.389-398, 1996.